Journal of Alloys and Compounds, *182* (1992) 145–156
JALCOM 147

Magnetic properties and ^{57}Fe Mössbauer spectroscopy of rare earth compounds of the type $RFe_{12-x}Co_xB_6$

M. Rosenberg, T. Sinnemann and M. Mittag
Experimentalphysik VI, Ruhr-Universität, 4630 Bochum (FRG)

K. H. J. Buschow
Philips Research Laboratories, 5600 JA Eindhoven (Netherlands)

(Received September 12, 1991)

Abstract

Compounds of the type $LaFe_{12-x}Co_xB_6$ were found to crystallize in the hexagonal $SrNi_{12}B_6$ structure type throughout the whole concentration range, the lattice constants decreasing linearly with x. The magnetic properties of these compounds were studied as a function of concentration. It was found that the 3d sublattice magnetization is very weak when $x < 8$, but increases substantially in compounds with $x \geqslant 8$ owing to ferromagnetic ordering. ^{57}Fe Mössbauer spectra for various $RFe_{12-x}Co_xB_6$ compounds were recorded in the temperature range 2.0–293 K. The iron concentrations considered were $x = 11.8$ for $R \equiv Y$ and Gd and $x \leqslant 10$ for $R \equiv La$. The average iron saturation hyperfine field decreases from 15.8 T ($x = 11.8$) to about 5 T in the pure iron compound. The ordering temperatures show a similar temperature dependence from 161 K for $x = 12$ to about 25 K for $x = 0$. Iron shows a strong site preference, so that in $YFe_{0.2}Co_{11.8}B_6$ 88% of the Fe atoms are located on one of the two transition metal sites. The iron hyperfine fields and quadrupole splittings corresponding to the two sites are markedly different.

1. Introduction

In a previous investigation it was shown that $NdFe_{12}B_6$ is a ferromagnet with a saturation magnetization of 125 A m^2 kg^{-1} and a Curie temperature of 230 K [1]. Its crystal structure is hexagonal ($SrNi_{12}B_6$ type) and of sufficiently low symmetry to give rise to a strong crystal-field-induced rare earth sublattice anisotropy. The low Curie temperature, however, means that this compound is not suitable for permanent-magnet purposes. The standard solution in such a case is to substitute cobalt for part of the iron, which has been shown to work well for a variety of different systems. This can be illustrated by means of Fig. 1, where the beneficial increase of T_c for several of such systems is shown [2–4]. At the same time, it can be seen from Fig. 1 that the system $Nd(Fe_{1-s}Co_s)_{12}B_6$ displays quite a different behaviour [5]. Instead of a Curie temperature enhancement, it is found that magnetic ordering seems to disappear altogether in the intermediate concentration range. In the present investigation an attempt will be made to find the origin of this deviating behaviour. For this purpose, we have studied the 3d sublattice

0925-8388/92/$5.00

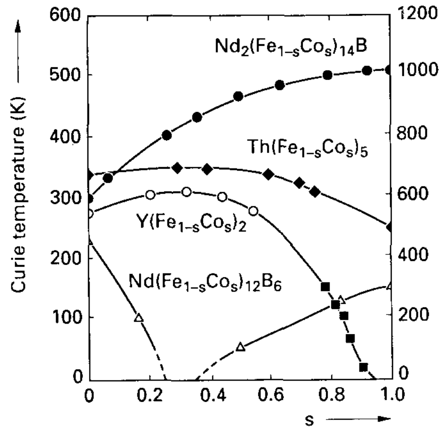

Fig. 1. Comparison of the concentration dependence of the Curie temperature in the systems $Nd_2(Fe_{1-s}Co_s)_{14}B$ (●), $Th(Fe_{1-s}Co_s)_5$ (◆), $Y(Fe_{1-s}Co_s)_5$ (○) (right-hand scale for all three) and $Nd(Fe_{1-s}Co_s)_{12}B_6$ (△) (left-hand scale).

magnetism in the series $LaFe_{12-x}Co_xB_6$ by means of magnetic measurements and ^{57}Fe Mössbauer spectroscopy.

2. Experimental details

The $RFe_{12-x}Co_xB_6$ samples were prepared by arc melting starting materials of at least 99% purity under purified argon gas, followed by vacuum annealing for 3 weeks at 900 °C. An X-ray diffraction analysis was carried out and the annealed samples were found to be approximately single phase for the cobalt-rich compositions. In the iron-rich compounds the amount of impurity phases was substantially larger, the main impurity phase being Fe_2B. The main diffraction lines were indexed on the basis of the hexagonal $SrNi_{12}B_6$ structure type with space group $R3m$. In this structure the R atoms occupy the 3a sites, whereas the 3d atoms reside on the 18h and 18g sites. The samples were ground into a spherical shape for the magnetic measurements, carried out in a sensitive vibrating-sample magnetometer in the temperature range 2.8–300 K and in fields up to 2 T. The saturation moments were obtained by extrapolating the values measured in the cryogenic range in high fields ($\mu_0H=1.75$ T) to $T=0$ K. The ordering temperatures were determined from measurements in low fields ($\mu_0H=1$ mT). In all cases the temperature dependence of the magnetization was measured after the samples had been cooled to 2.8 K in the presence of a magnetic field. ^{57}Fe Mössbauer spectra were recorded in the temperature range 2.0–293 K. Besides 1–2% α-Fe, another contamination with a temperature-independent hyperfine field of 23–25 T showed up in all spectra of the iron-rich compounds. The corresponding subspectrum had well-defined parameters and belongs most likely to Fe_2B [6]. Its contribution can easily be subtracted from the other data during the fitting procedure and therefore does not influence the results.

The Fe_2B content was found to amount to 24%, 11%, 8% and 4% for $x=0$, 2, 4 and 5 respectively in $LaFe_{12-x}Co_xB_6$ and less than 2% in all other compounds, including $GdCo_{12}B_6$ and $YCo_{12}B_6$ doped with 2% of enriched ^{57}Fe.

3. Experimental results

3.1. *X-ray diffraction*

The lattice constants derived from the X-ray diffraction analysis have been plotted as a function of concentration in Fig. 2. It can be seen that Vegard's law is followed, both lattice parameters decreasing linearly with increasing cobalt concentration.

3.2. *Magnetic measurements*

The temperature dependence of the magnetization of the $LaFe_{12-x}Co_xB_6$ compounds investigated is shown in Fig. 3. It has already been mentioned in the previous section that considerable amounts of impurities are present in the iron-rich samples. The reason for this is the difficulty with which compounds of the type $RFe_{12}B_6$ form. In fact, $LaFe_{12}B_6$ is the only representative of the latter series that we were able to prepare when using standard arc melting and annealing. Attempts to prepare other members of this series failed. Here we recall that the compound $NdFe_{12}B_6$ reported earlier [1] had been prepared via the amorphous state, using melt spinning followed by a heat treatment.

The amounts of impurity phases present in the samples could readily be estimated from the high-temperature behaviour of the magnetization, since all of the impurity phases (Co_2B or Fe_2B) have Curie temperatures considerably

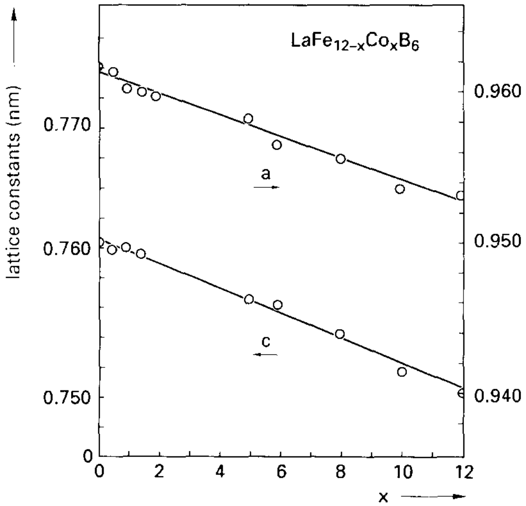

Fig. 2. Concentration dependence of the lattice constants in the system $LaFe_{12-x}Co_xB_6$.

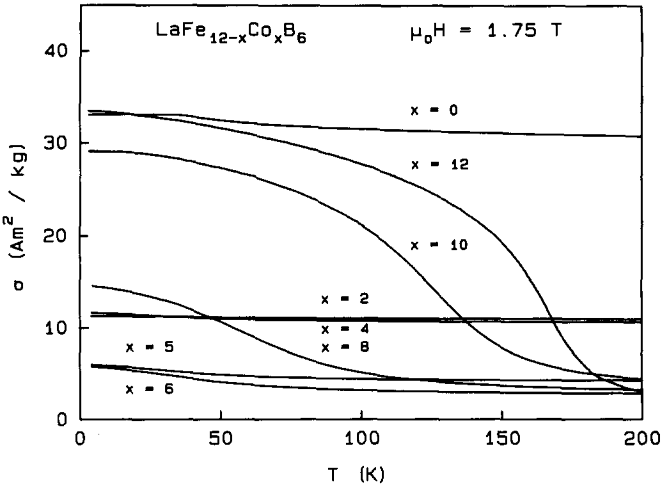

Fig. 3. Temperature dependence of the magnetization in samples of the type $LaFe_{12-x}Co_xB_6$ before correction for the contribution of impurity phases (μ_0H=1.75 T).

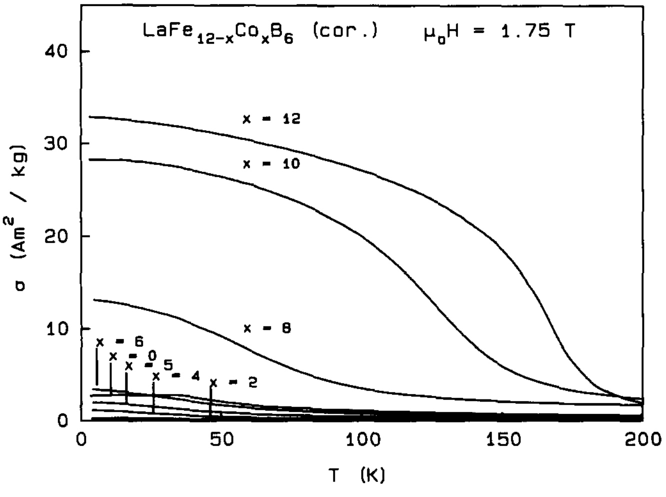

Fig. 4. Temperature dependence of the magnetization in samples of the type $LaFe_{12-x}Co_xB_6$ after correction for the contribution of impurity phases (μ_0H=1.75 T).

in excess of those of the $LaFe_{12-x}Co_xB_6$ compounds. The amounts of impurities estimated in this manner correspond closely to those found from Mössbauer spectroscopy (see below). The temperature dependence of the magnetization of the various samples $LaFe_{12-x}Co_xB_6$ after correction for the impurity phase is shown in Fig. 4. It follows from these results that the ferromagnetic character of the $LaFe_{12-x}Co_xB_6$ compounds is largely lost when the iron concentration is close to $x=6$ or lower.

3.3. ^{57}Fe Mössbauer spectroscopy

In the paramagnetic region, all spectra could be fitted with two doublets. The typical linewidth of 0.28 mm s^{-1} used did not exceed the instrumental linewidth. Since the line positions in the positive velocity range are not unique, two fits of equal quality are possible (see Fig. 5), leading to two sets of isomer shifts (ISs) and quadrupole splittings (QSs). The two interpretations of the spectra can be characterized as follows: A, "inside–outside doublets" with approximately equal IS and different QSs; B, "left–right doublets" with different ISs and approximately equal QS.

In $YCo_{11.8}Fe_{0.2}B_6$, only interpretation A leads to a good fit. For this reason we will leave interpretation B out of consideration. The concentration dependence of the quadrupole splitting for interpretation A of the spectra is plotted in Fig. 6.

The average ISs increase from about 0.01 mm s^{-1} in $LaFe_{12}B$ to 0.08 mm s^{-1} in $RCo_{11.8}Fe_{0.2}B_6$ (see Fig. 7), the separate IS values of the two doublets showing an analogous behaviour. This trend is different from that observed when substituting iron into cobalt metal (IS = -0.04 mm s^{-1} [7]) or into $Nd_2Co_{14}B$ [8] (where the average value becomes smaller than in $Nd_2Fe_{14}B$ [9] by about -0.1 mm s^{-1}).

The relative intensities of the two doublets can be determined with good precision because of the marked structure of the spectra in the negative velocity range (for completeness we note that both fitting procedures, A and B, gave identical results). In $LaFe_{12}B_6$, the two doublets have the same intensity as expected on the basis of the crystal structure. However, for lower iron concentrations, the Fe atoms show a strong site preference. For

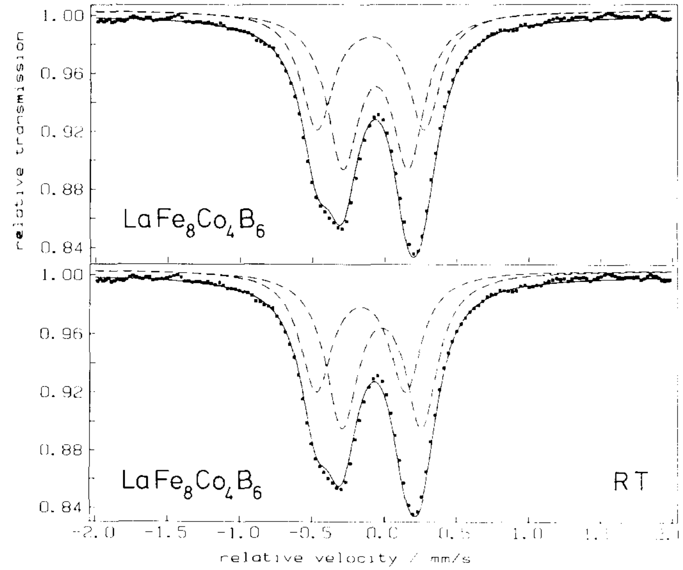

Fig. 5. ^{57}Fe Mössbauer spectra of $LaFe_8Co_4B_6$ at room temperature. The top and bottom parts show the fitting according to method A and method B respectively described in the main text.

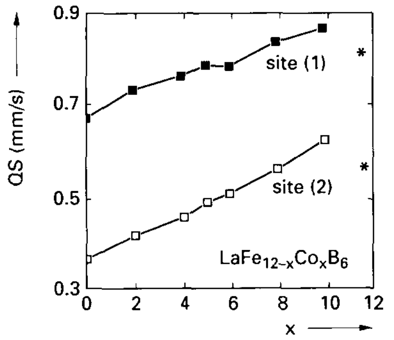

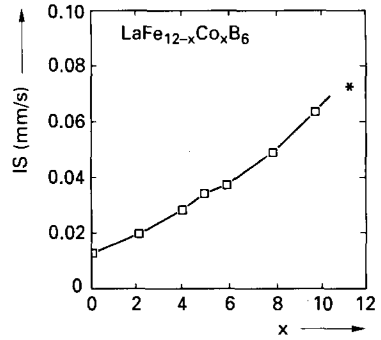

Fig. 6. QS of the ^{57}Fe Mössbauer spectra of $LaFe_{12-x}Co_xB_6$ compounds at room temperature (■, □): *, data obtained on $YFe_{0.2}Co_{10.8}B_6$. The data pertaining to the two subspectra are denoted by site 1 and site 2.

Fig. 7. Concentration dependence of the average isomer shift in the ^{57}Fe Mössbauer spectra of $LaFe_{12-x}Co_xB_6$ (□) and $YFe_{0.2}Co_{11.8}B_6$ (*) at room temperature.

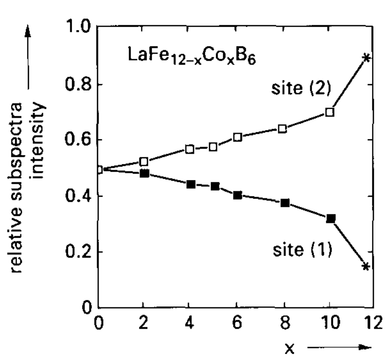

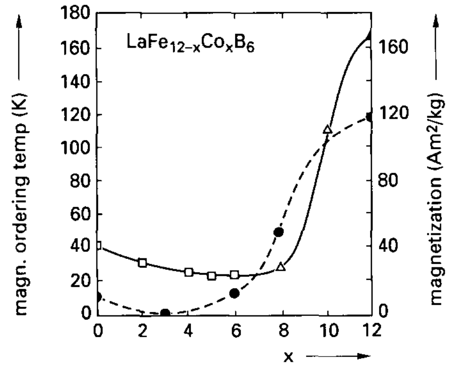

Fig. 8. Relative intensity of the two subspectra of $LaFe_{12-x}Co_xB_6$ (■, □) and $YFe_{0.2}Co_{10.8}B_6$ (*). The same notation of the sites is used as in Fig. 6.

Fig. 9. Magnetic ordering temperatures in $LaFe_{12-x}Co_xB_6$ derived from the onset of magnetic broadening of the ^{57}Fe Mössbauer spectra (□) and as obtained from magnetic measurements (△): ●, the concentration dependence of the magnetization.

instance, in $YCo_{11.8}Fe_{0.2}B_6$ about 88% of the Fe atoms are located in one of the two transition metal sites. In $GdCo_{11.8}Fe_{0.2}B_6$ the corresponding value is 82%. The concentration dependence of the relative subspectra intensities is shown in Fig. 8. The lower curve in Fig. 8 corresponds to the subspectrum with the higher QS.

At lower temperatures broadening of the paramagnetic doublet occurs, which is due to Zeeman splitting of the spectra, associated with magnetic ordering. The Curie temperatures of the compounds $LaFe_{12-x}Co_xB_6$ ($x=6$, 5, 4, 2, 0) were determined as the points where broadening of the paramagnetic doublets sets in. The results have an accuracy of ±5 K and are plotted in Fig. 9.

The Mössbauer spectra at 4.2 K for the compounds with $x \geqslant 4$ can be described as magnetically broadened rather than as magnetically split. Unfortunately, an approach in which magnetic and electric interactions are of the same order of magnitude cannot be applied here as a basis for fitting the spectra because of lack of structure. Nevertheless, in order to obtain a rough estimate of the average hyperfine fields, we took the average over four sextets (the number was chosen arbitrarily) of equal intensity. The result is essentially the same as if we had measured the overall width of the spectra. Decreasing the temperature to 2.0 K for the compounds with $x = 6$, 5, 4, 2 and 0 leaves their spectra unchanged. The values of the average hyperfine fields determined in this way have the same concentration dependence as the Curie temperatures, as may be seen from Fig. 10. Note that the minimum at $x = 4$ and $x = 2$ is not an artefact of the fitting procedure, as can be inferred from visual inspection of the Mössbauer spectra shown in Fig. 11.

The hyperfine fields at 4.2 K, corresponding to the two transition metal sites, can be determined separately in the spectra of the two $RFe_{0.2}Co_{11.8}B_6$ compounds investigated. The spectrum of $GdFe_{0.2}Co_{11.8}B_6$ is shown in Fig. 12. The outer regions of the spectra can be fitted with three sextets of approximately equal intensity, with hyperfine field values of 14.8, 15.7 and 16.7 T ($R \equiv Gd$) and 14.3, 15.3 and 16.5 T ($R \equiv Y$). The intensity of these subspectra in the low velocity range (central region) is fixed within a certain limit, because the intensity ratio 3:2:1:1:2:3 for the six lines of a sextet in a thin absorber can become shifted to no more than approximately 3:2.4:1.3:1.3:2.4:3 in a normal absorber. In the low velocity region, we measure, however, significantly more intensity than expected, even when taking the maximum possible intensity shift into consideration. In fact, fitting the spectrum for $R \equiv Y$ with only the three sextets mentioned above would lead to an unrealistic intensity ratio of 3:2.3:2.3:2.3:3. This can only be explained by the presence of an additional subspectrum. This subspectrum has to be attributed to the 12% ($R \equiv Y$) or 18% ($R \equiv Gd$) of the Fe atoms

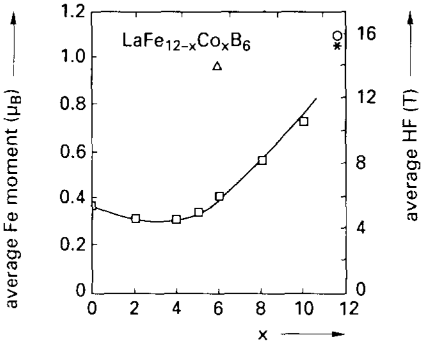

Fig. 10. Average value of the hyperfine field derived from fitting the ^{57}Fe Mössbauer spectra of $LaFe_{12-x}Co_x$ measured at 4.2 K (□). Data obtained for $YFe_{0.2}Co_{11.8}B_6$ (∗) and $GdFe_{0.2}Co_{11.8}B_6$ (○) are also shown.

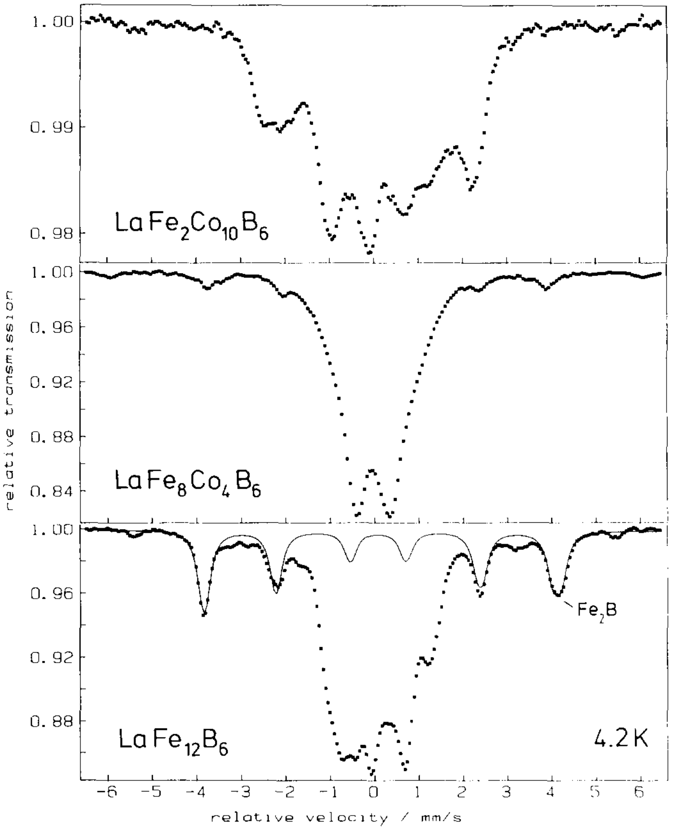

Fig. 11. Comparison of ^{57}Fe Mössbauer spectra at 4.2 K for $LaFe_{12-x}Co_xB_6$ compounds with $x = 10$ (top), $x = 4$ (middle) and $x = 0$ (bottom). In the bottom spectrum the relative contribution of the impurity subspectrum (Fe_2B) is shown.

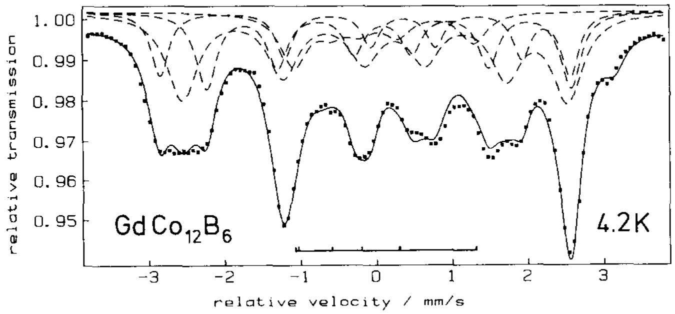

Fig. 12. ^{57}Fe Mössbauer spectrum of $GdCo_{12}B_6$ doped with 2% Fe enriched in ^{57}Fe. The decomposition of the spectrum into its main components (as described in the main text) is shown at the top of the figure. The line positions of the subspectrum having the lowest hyperfine splitting are indicated at the bottom.

located on the second of the two available 3d atom sites, as was derived already from the room temperature spectra. When using a reasonable intensity ratio for the six lines of the sextets of the three subspectra discussed above, we find that fitting of the 4.2 K spectra leads to a subspectrum (14%) with a hyperfine field value of about 3 ± 2 T for R≡Y and to a subspectrum (15%) with a hyperfine field value of about 7.5 ± 2 T for R≡Gd.

The occurrence of the hyperfine fields differing by a factor of more than 2 for the two lattice sites is supported by NMR measurements on $RCo_{12}B_6$ with R≡Y, Gd [10] and R≡Nd [11], the corresponding ^{59}Co hyperfine fields being 3.3 and 7.5 T (in $YCo_{12}B_6$).

As already mentioned above, we have assigned the three equally populated sextets with hyperfine field values differing by 1 T to only a single lattice site. According to the calculation of Erdmann *et al.* [10], an easy magnetization direction lying in the basal plane would split a given 3d metal lattice site into several magnetically inequivalent positions. This may be caused by dipolar fields. However, especially in the yttrium-based compound, these fields are much too small to account for the observed difference. Alternatively, it may be caused by anisotropic orbital contributions, for which differences in iron site hyperfine fields of about 1 T are of the right order of magnitude [12].

4. Discussion

It was mentioned already in the Introduction that the concentration dependence of the Curie temperature of the compounds $NdCo_{12-x}Fe_xB_6$ is rather unusual and leads to a minimum rather than to a maximum, as observed in several other series of compounds (Fig. 1). The results obtained in the present investigation on $LaCo_{12-x}Fe_xB_6$ have shown that a similar behaviour is found also in the latter system. The present results have also provided a clue that the origin of the weakening of the magnetism in these materials originates from the iron sublattice, which in $LaFe_{12}B_6$ is different from that in the other iron compounds shown in Fig. 1. This will be discussed in more detail below.

In the first place it is worth noting that the hyperfine splitting in $LaFe_{12}B_6$ at 2 K is very low. The average hyperfine splitting equals 6 T at this temperature. When using the hyperfine coupling constant close to 14.5 T μ_B^{-1}, as found in many other R–Fe compounds [13, 14], one derives an average moment value of $0.35\mu_B$ per Fe atom (shown also in Fig. 10). In view of the uncertainties associated with the rather low hyperfine splitting of the Mössbauer spectra, this average moment value has probably to be regarded as an upper limit. This low moment value is accompanied by a fairly low magnetic ordering temperature, close to 40 K, as may be seen in Fig. 9. The results shown in Fig. 4 suggest that the ordering is not of the ferromagnetic type, the maximum in the $\sigma(T)$ curve being more indicative of antiferromagnetism or of a spin glass type of ordering. All these properties are in strong contrast to those found in $NdFe_{12}B_6$. The latter compound is ferromagnetic with $T_c = 230$ K and a saturation moment at 4.2 K of $19.7\mu_B$ per formula unit. After subtracting $3.3\mu_B$ for the free ion value of the neodymium moment, one derives a total iron sublattice moment of $16.4\mu_B$, leading to an average iron moment of $1.37\mu_B$. These results show that the presence of the polarizing rare earth spin has led to an enhancement of the iron sublattice moment by about 400%. Rare-earth-spin-induced enhancements of the iron sublattice in other R–Fe compounds are generally much lower and remain below 30% even in the RFe_2 series [15]. The results suggest that $LaFe_{12}B_6$ is a compound in which the iron sublattice moment is close to collapsing. Since it is well known that lattice contraction generally has a detrimental influence on iron moment formation, it is likely that cobalt substitution into $LaFe_{12}B_6$ (see Fig. 2) further decreases the iron sublattice magnetization, overcompensating any spin-polarizing influence of the cobalt moments. This may explain the initial decrease of the average values of hyperfine field and μ_{Fe} when proceeding from left to right in Fig. 10.

From the concentration dependence of the intensities of the subspectra corresponding to the two crystallographic 3d sites in $R(Fe,Co)_{12}B_6$ it is possible to calculate the concentration dependence of the cobalt and iron site occupation. Results obtained for the cobalt site occupation are shown in Fig. 13. The broken line represents the ideal site occupation, *i.e.* when any site preference is absent. The lower curve (site 2) is to be associated with the site 2 curve in Fig. 8, the corresponding site being preferentially occupied by Fe atoms. The upper curve (site 1) corresponds to the curve denoted by site 1 in Fig. 8. It pertains to the site that is largely avoided by the Fe atoms or, alternatively, is preferentially occupied by Co atoms. By combining previous results of ^{59}Co NMR on $Y_2Co_{12}B_6$ [10] with ^{57}Fe Mössbauer spectroscopy obtained in the course of the present investigation on $YCo_{11.8}Fe_{0.2}B_6$, one finds that site 2 favours a high 3d moment and gives rise to a modest quadrupole splitting, while at site 1 the 3d moment is much lower and the quadrupolar splitting much higher.

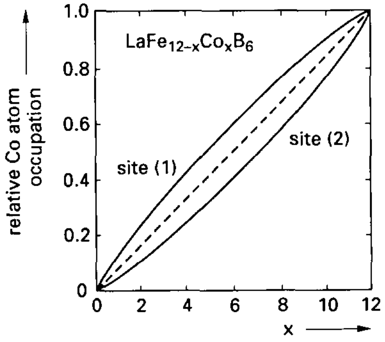

Fig. 13. Relative cobalt atom occupation of the two available crystallographic 3d sites in $LaFe_{12-x}Co_xB_6$: – —, statistical site occupation of iron and cobalt.

Although this will not strictly be necessary for our interpretation, one may associate site 2 with the 18h position characterized by nine transition metal neighbours and three boron neighbours. Site 1 has then to be associated with the 18g position, surrounded by only seven transition metal neighbours and four boron atoms.

Proceeding from the left site of Fig. 13, one finds that cobalt substitution in $LaFe_{12}B_6$ initially takes place predominantly into site 1. Since this site is less favourable for 3d moment formation, it is doubtful whether the Co atoms will acquire a magnetic moment in the cobalt-poor concentration regime. Site 2 becomes occupied by Co atoms considerably more slowly. This site is primarily responsible for the cobalt sublattice magnetization ($0.7\mu_B$ per Co atom compared with $0.3\mu_B$ per Co atom for the other site [10]) and there is a concomitant strong rise in overall magnetization in the cobalt-rich regime of the system $LaFe_{12-x}Co_xB_6$ (Fig. 9).

5. Concluding remarks

We have shown that a stable compound of the composition $LaFe_{12}B_6$ with $SrNi_{12}B_6$ structure exists. In this compound the Fe atoms adopt rather low moment values ($0.35\mu_B$) and the ordering temperature is also fairly low (40 K). This compound can be regarded as being close to moment instability and a strong moment enhancement occurs when lanthanum is replaced by a magnetic rare earth atom. The unstable character of the iron moment in $LaFe_{12-x}Co_xB_6$ is probably the reason why this system behaves differently from other systems in which cobalt is substituted for iron, such as $Y(Fe_{1-x}Co_x)_2$, $Th(Fe_{1-x}Co_x)_5$ or $Nd_2(Fe_{1-x}Co_x)_{14}B$. In all the latter cases the iron moments are stable and the 3d sublattice magnetization gives rise to a maximum, while the magnetic ordering temperature increases even when the pure cobalt compound is non-magnetic (YCo_2). The fact that the 3d sublattice moment almost collapses in the intermediate concentration of $LaFe_{12-x}Co_xB_6$ is partly due to preferential site occupation, the Co atoms going into the 3d site that is less favourable for 3d moment formation.

References

1 K. H. J. Buschow, D. B. de Mooij and H. M. van Noort, *J. Less-Common Met.*, *125* (1986) 135.

2 M. G. Luipen, P. C. M. Gubbens, A. M. van der Kraan, J. J. van Loef and K. H. J. Buschow, unpublished results.

3 W. Steiner and H. Ortbauer, *Phys. Status Solidi*, *26* (1974) 45.

4 A. M. van Diepen, K. H. J. Buschow and J. S. van Wieringen, *J. Appl. Phys.*, *43* (1971) 645.

5 K. H. J. Buschow, in C. Herget and R. Poerschke (eds.), *Proc. 9th Int. Workshop on Rare Earth Magnets, Bad Soden*, Deutsche Physikalische Gesellschaft GmbH, Bad Honnef, 1987, pp. 453.

6 K. Murphy and N. Hershkowitz, *Phys. Rev. B*, *7* (1973) 23.

7 S. M. Qaim, *Proc. Phys. Soc., London, 90* (1967) 1065.

8 H. M. van Noort and K. H. J. Buschow, *J. Less-Common Met., 113* (1985) L9.

9 H. M. van Noort, D. B. de Mooij and K. H. J. Buschow, *J. Appl. Phys., 57* (1985) 5414.

10 K. Erdmann, M. Rosenberg and K. H. J. Buschow, *J. Appl. Phys., 63* (1988) 4113.

11 Cz. Kapusta, personal communication, 1990.

12 R. J. Zhou, T. Sinnemann, M. Rosenberg and K. H. J. Buschow, *J. Less-Common Met., 171* (1991) 263.

13 T. Sinnemann, K. Erdmann, M. Rosenberg and K. H. J. Buschow, *Hyperfine Interactions, 50* (1989) 375.

14 P. C. M. Gubbens, J. H. J. van Apeldoorn, A. M. van der Kraan and K. H. J. Buschow, *J. Phys. F, 4* (1974) 921.

15 M. S. S. Brooks, L. Nordström and B. Johansson, *J. Phys.: Condens. Matter., 3* (1991) 2357.